Lattice Boltzmann method for the compressible Euler equations

Takeshi Kataoka* and Michihisa Tsutahara
Graduate School of Science and Technology, Kobe University, Rokkodai, Nada, Kobe 657-8501, Japan
(Received 28 November 2003; published 18 May 2004)

The lattice Boltzmann model for the compressible Euler equations is proposed together with its rigorous theoretical background. The proposed model has completely overcome the defects of the previous model that the specific-heat ratio cannot be chosen freely. The macroscopic variables obtained from the solution are shown to satisfy, in the limit of the small Knudsen number, the compressible Euler equations if the variation of the solution is moderate. This is the case where no shock waves or contact discontinuities appear. In contrast, when the solution makes steep variation at several localized regions due to the appearance of shock waves and contact discontinuities, the corresponding macroscopic variables satisfy the weak form of the Euler equations. Their derivation is carried out rigorously by taking into account the scale of variation of the solution correctly. This is the first study that has laid the theoretical foundation of the lattice Boltzmann model for the simulation of flows with shock waves and contact discontinuities. Numerical examples and the error estimates are also given, which are consistent with the above theoretical arguments.

DOI: 10.1103/PhysRevE.69.056702 PACS number(s): 02.70.Ns, 47.11.+j, 47.40.−x

I. INTRODUCTION

Recently, the lattice Boltzmann method (LBM) is attracting a great deal of attention [1–9]. The LBM solves the kinetic equation of the discrete-molecular-velocity type such that the macroscopic variables obtained from the solution satisfy the desired fluid-dynamics-type equations. Various merits of the LBM are pointed out: a simple scheme, linear advective terms, high resolution for shock wave computation, and so on. Because of the last merit for the shock wave computation, the LBM is often used as a simulation tool for compressible flows with shock waves and contact discontinuities [1–3]. However, its theoretical background is unclear. We focus on this aspect first, and then make a statement about our model subsequently.

When using the LBM as a numerical tool, one must confirm that the macroscopic variables obtained from the solution of the kinetic equation of the LBM satisfy the desired fluid-dynamic-type equations in the limit of $\varepsilon \to 0$, where ε is the Knudsen number. For that purpose, the so-called Chapman-Enskog expansion is often used [1–8]. Recently, as the more systematic analytical procedure, the asymptotic analysis is also used [9]. We must note, however, that such analytical confirmation makes sense only when the numerical scheme used in the LBM is consistent with the original kinetic equation. That is, the difference between the numerical scheme and the original kinetic equation must remain small. Otherwise, the theoretical confirmation of the LBM starting from the original kinetic equation is meaningless.

Bearing this in mind, let us consider flows with shocks and contact discontinuities, which are of our interest in the present study. It is known that the dimensionless width of shocks and contact discontinuities is of the order of ε according to the kinetic theory [10,11]. In order to assure the consistency of the numerical scheme, therefore, it must satisfy the severe restriction that the dimensionless mesh width is much smaller than ε, since the kinetic equation involves derivative terms. The derivative terms can generate error terms of finite magnitude if the mesh width is $O(\varepsilon)$, or the width of the shocks or the contact discontinuities.

However, the mesh width of $O(\varepsilon)$ is often used to simulate flows with shocks and contact discontinuities by the LBM in order to save computation time [1–3]. It is imperative, therefore, to present a clear theoretical background. To this end, we consider the integral relation of the kinetic equation in the same manner as the weak form of the Euler equations being considered when treating solutions with discontinuities [12–15]. This integral relation includes no derivatives of the velocity distribution function. It is easy to show that, even if the mesh width is $O(\varepsilon)$, the usual finite-difference scheme of the kinetic equation is consistent with this integral relation (the proof is shown in the Appendix of the present study). We then prove that the macroscopic variables obtained from the solution of this integral relation satisfy, in the limit of $\varepsilon \to 0$, the weak form of the compressible Euler equations. It is well known that the weak form of the compressible Euler equations can correctly describe flows with shocks and contact discontinuities if the subsidiary entropy condition is satisfied [13–15].

In addition, we present a new lattice Boltzmann model that gives the solutions of the compressible Euler equations (and also their weak form). In the early models [2–4], there was a serious defect that the specific-heat ratio cannot be chosen freely. Recently, the two-dimensional model that overcomes this defect was suggested [1]. The new model presented in this study, however, is not limited to the two-dimensional version, but also for the one- and three-dimensional versions. Moreover, the new model of the two-dimensional version succeeded in reducing the number of molecular velocities from 17 of the previous model to 9. Thus, the computation time is almost halved. The other dimensional versions are also small in their number of molecu-

*Corresponding author. FAX: +81-78-803-6137; Email address: kataoka@mech.kobe-u.ac.jp

lar velocities (5 and 15 for the one- and the three-dimensional versions, respectively).

It is noted here that the compressible Navier-Stokes (NS) equations are not necessary for the analysis of the initial-value problem of compressible flows in their continuum limit (or flows whose Mach number is of the order of unity in their continuum limit $\varepsilon \to 0$). In the compressible flows, the viscous and diffusive terms appear only as perturbations of the Euler equations and they vanish in the continuum limit [16,17]. Therefore, the lattice Boltzmann model for the Euler equations is sufficient to describe compressible flows. It is inefficient to use the lattice Boltzmann model for the compressible NS equations [18] whose number of molecular velocities and computation time become larger in general.

The present paper is arranged in the following order. In Sec. II, the new lattice Boltzmann model is presented. Its theoretical background is given in Sec. III, where the asymptotic analysis for small ε is carried out. Numerical examples and error estimates are arranged in Sec. IV. In the last section (Sec. V), some concluding remarks are given.

II. LATTICE BOLTZMANN MODEL

We introduce a lattice Boltzmann model in its dimensional form in Sec. II A, and then, in its nondimensional form in Sec. II B.

A. Dimensional expressions

First, we write down the compressible Euler equations explicitly:

$$\frac{\partial \rho}{\partial t} + \frac{\partial \rho u_\alpha}{\partial x_\alpha} = 0, \tag{1a}$$

$$\frac{\partial \rho u_\alpha}{\partial t} + \frac{\partial \rho u_\alpha u_\beta}{\partial x_\beta} + \frac{\partial p}{\partial x_\alpha} = 0, \tag{1b}$$

$$\frac{\partial \rho(bRT + u_\alpha^2)}{\partial t} + \frac{\partial \rho u_\alpha (bRT + u_\beta^2) + 2pu_\alpha}{\partial x_\alpha} = 0 \tag{1c}$$

$$(\alpha = 1,2,\ldots,D; \quad \beta = 1,2,\ldots,D),$$

where t is the time, x_α is the spatial coordinate, ρ, u_α, T, and

$$p = \rho RT \tag{2}$$

are, respectively, the density, the flow velocity in the x_α direction, the temperature, and the pressure of a gas. R and D are the specific gas constant and the number of spatial dimensions, respectively. b is a given constant expressed as

$$b = \frac{2}{\gamma - 1}, \tag{3}$$

where γ is the specific-heat ratio. Note that, in the present study, the subscripts α and β represent the number of spatial coordinates and the summation convention is applied to these subscripts. The initial condition is

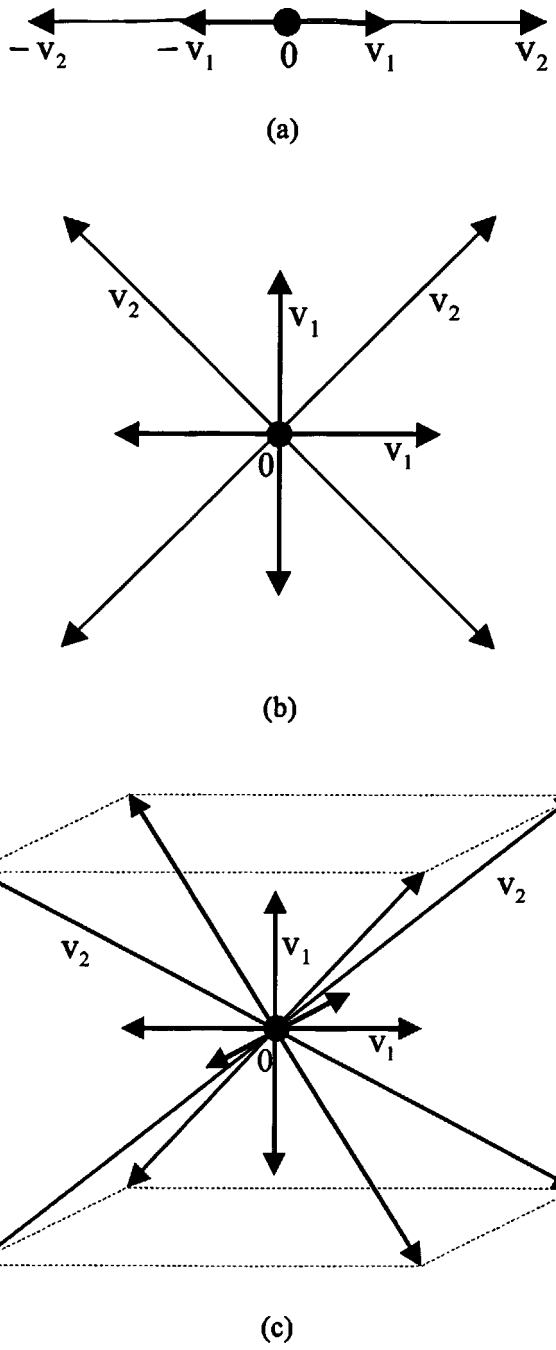

FIG. 1. Distribution of the discrete molecular velocities $c_{i\alpha}(\alpha = 1,\ldots,D; i = 1,2,\ldots,I)$ for each dimensional model: (a) one-dimensional model ($D=1, I=5$); (b) two-dimensional model ($D=2, I=9$); (c) three-dimensional model ($D=3, I=15$).

$$\rho = \rho^0, \quad u_\alpha = u_\alpha^0, \quad T = T^0 \quad \text{at} \quad t = 0, \tag{4}$$

where ρ^0, u_α^0, and T^0 are given functions of x_α.

Now we present a lattice Boltzmann model that gives the solutions of the initial-value problem of the compressible Euler equations (1a)–(1c) with the initial condition (4). Let $c_{i\alpha}$ ($i = 1,2,\ldots,I$; I is the total number of discrete molecular velocities) be the molecular velocity in the x_α direction of the ith particle, and η_i be another variable newly introduced to

control the specific-heat ratio. $f_i(t,x_\alpha)$ is the velocity distribution function of the ith particle. The macroscopic variables ρ, u_α, and T are defined as

$$\rho = \sum_{i=1}^{I} f_i, \tag{5a}$$

$$\rho u_\alpha = \sum_{i=1}^{I} f_i c_{i\alpha}, \tag{5b}$$

$$\rho(bRT + u_\alpha^2) = \sum_{i=1}^{I} f_i(c_{i\alpha}^2 + \eta_i^2). \tag{5c}$$

Note that, in the present study, the summation convention is not applied to the subscript i representing the kind of molecules.

Consider the initial-value problem of the Bhatnager—Gross-Krook-type kinetic equation [19]:

$$\frac{\partial f_i}{\partial t} + c_{i\beta}\frac{\partial f_i}{\partial x_\beta} = \frac{f_i^{\mathrm{eq}}(\rho,u_\alpha,T) - f_i}{\tau}, \tag{6}$$

with the initial condition

$$f_i = f_i^{\mathrm{eq}}(\rho^0,u_\alpha^0,T^0) \quad \text{at} \quad t = 0, \tag{7}$$

where τ (the relaxation time) is a given constant and $f_i^{\mathrm{eq}}(\rho,u_\alpha,T)$ (the local equilibrium velocity distribution function) is a given function of the macroscopic variables. In the LBM, the following discretized form of Eq. (6) is often used:

$$\frac{f_i(t+\Delta t, x_\alpha + c_{i\alpha}\Delta t) - f_i(t,x_\alpha)}{\Delta t} = \frac{f_i^{\mathrm{eq}}(\rho,u_\alpha,T) - f_i}{\tau}, \tag{8}$$

where Δt is the discrete time step of order τ. It is clear that Eq. (8) is only one of the finite-difference scheme of the kinetic equation (6). Therefore, we use Eq. (6) as a basic kinetic equation in the following. It is also noted that there is a recent trend in the LBM community to use the usual finite-difference scheme of Eq. (6) rather than Eq. (8) due to the numerical stability problem [20,21].

Now return to the explanation of the lattice Boltzmann models. The following constraints are imposed on the moments of f_i^{eq} appearing on the right-hand sides of Eqs. (6) and (7):

$$\rho = \sum_{i=1}^{I} f_i^{\mathrm{eq}}, \tag{9a}$$

$$\rho u_\alpha = \sum_{i=1}^{I} f_i^{\mathrm{eq}} c_{i\alpha}, \tag{9b}$$

$$p\delta_{\alpha\beta} + \rho u_\alpha u_\beta = \sum_{i=1}^{I} f_i^{\mathrm{eq}} c_{i\alpha} c_{i\beta}, \tag{9c}$$

$$\rho(bRT + u_\alpha^2) = \sum_{i=1}^{I} f_i^{\mathrm{eq}}(c_{i\alpha}^2 + \eta_i^2), \tag{9d}$$

$$\rho[(b+2)RT + u_\beta^2]u_\alpha = \sum_{i=1}^{I} f_i^{\mathrm{eq}}(c_{i\beta}^2 + \eta_i^2)c_{i\alpha}, \tag{9e}$$

Then the macroscopic variables ρ, u_α, and T derived from the solution of the kinetic equation (6) with the initial condition (7) satisfy the compressible Euler equations (1a)–(1c) and their initial condition (4) if the time and length scales of variation of solution are much larger than τ and $\tau\sqrt{RT}$, respectively. The proof is given in Sec. III A.

The specific models that satisfy the above constraints (9a)–(9e) are presented in the following section (Sec. II B).

B. Nondimensional expressions

The nondimensional variables and equations, which are convenient for the following analysis and numerical calculation, are listed first.

Let L, ρ_0, and T_0 be, respectively, the reference length, density, and temperature. Then, the nondimensional variables are defined as follows:

$$\hat{t} = \frac{t}{L/\sqrt{RT_0}}, \quad \hat{x}_\alpha = \frac{x_\alpha}{L}, \quad \hat{c}_{i\alpha} = \frac{c_{i\alpha}}{\sqrt{RT_0}}, \quad \hat{\eta}_i = \frac{\eta_i}{\sqrt{RT_0}},$$

$$\hat{f}_i = \frac{f}{\rho_0}, \quad \hat{f}_i^{\mathrm{eq}} = \frac{f_i^{\mathrm{eq}}}{\rho_0},$$

$$\hat{\rho} = \frac{\rho}{\rho_0}, \quad \hat{u}_\alpha = \frac{u_\alpha}{\sqrt{RT_0}}, \quad \hat{T} = \frac{T}{T_0}, \quad \hat{p} = \frac{p}{\rho_0 RT_0},$$

$$\hat{\rho}^0 = \frac{\rho^0}{\rho_0}, \quad \hat{u}_\alpha^0 = \frac{u_\alpha^0}{\sqrt{RT_0}}, \quad \hat{T}^0 = \frac{T^0}{T_0}, \quad \hat{p}^0 = \frac{p^0}{\rho_0 RT_0}. \tag{10}$$

In terms of these nondimensional variables, the compressible Euler equations (1a)–(1c) and their initial condition (4) are

$$\frac{\partial \hat{\rho}}{\partial \hat{t}} + \frac{\partial \hat{\rho}\hat{u}_\alpha}{\partial \hat{x}_\alpha} = 0, \tag{11a}$$

$$\frac{\partial \hat{\rho}\hat{u}_\alpha}{\partial \hat{t}} + \frac{\partial \hat{\rho}\hat{u}_\alpha\hat{u}_\beta}{\partial \hat{x}_\beta} + \frac{\partial \hat{p}}{\partial \hat{x}_\alpha} = 0, \tag{11b}$$

$$\frac{\partial \hat{\rho}(b\hat{T} + \hat{u}_\alpha^2)}{\partial \hat{t}} + \frac{\partial \hat{\rho}\hat{u}_\alpha(b\hat{T} + \hat{u}_\beta^2) + 2\hat{p}\hat{u}_\alpha}{\partial \hat{x}_\alpha} = 0 \tag{11c}$$

$$(\alpha = 1,2,\ldots,D; \quad \beta = 1,2,\ldots,D),$$

where

$$\hat{p} = \hat{\rho}\hat{T} \tag{12}$$

and

$$\hat{\rho} = \hat{\rho}^0, \quad \hat{u}_\alpha = \hat{u}^0_\alpha, \quad \hat{T} = \hat{T}^0 \quad \text{at} \quad \hat{t} = 0. \tag{13}$$

The nondimensional macroscopic variables used in the LBM are defined as

$$\hat{\rho} = \sum_{i=1}^{I} \hat{f}_i, \tag{14a}$$

$$\hat{\rho}\hat{u}_\alpha = \sum_{i=1}^{I} \hat{f}_i \hat{c}_{i\alpha}, \tag{14b}$$

$$\hat{\rho}(b\hat{T} + \hat{u}^2_\alpha) = \sum_{i=1}^{I} \hat{f}_i(\hat{c}^2_{i\alpha} + \hat{\eta}^2_i), \tag{14c}$$

from Eqs. (5a)–(5c). The kinetic equation (6) and its initial condition (7) of nondimensional form are

$$\frac{\partial \hat{f}_i}{\partial \hat{t}} + \hat{c}_{i\beta}\frac{\partial \hat{f}_i}{\partial \hat{x}_\beta} = \frac{\hat{f}^{\mathrm{eq}}_i(\hat{\rho}, \hat{u}_\alpha, \hat{T}) - \hat{f}_i}{\varepsilon}, \tag{15}$$

and

$$\hat{f}_i = \hat{f}^{\mathrm{eq}}_i(\hat{\rho}^0, \hat{u}^0_\alpha, \hat{T}^0) \quad \text{at} \quad \hat{t} = 0, \tag{16}$$

where ε is the Knudsen number defined by

$$\varepsilon = \frac{\tau\sqrt{RT_0}}{L}. \tag{17}$$

$\hat{f}^{\mathrm{eq}}_i$ satisfies the following constraints from Eqs. (9a)–(9e):

$$\hat{\rho} = \sum_{i=1}^{I} \hat{f}^{\mathrm{eq}}_i, \tag{18a}$$

$$\hat{\rho}\hat{u}_\alpha = \sum_{i=1}^{I} \hat{f}^{\mathrm{eq}}_i \hat{c}_{i\alpha}, \tag{18b}$$

$$\hat{p}\delta_{\alpha\beta} + \hat{\rho}\hat{u}_\alpha\hat{u}_\beta = \sum_{i=1}^{I} \hat{f}^{\mathrm{eq}}_i \hat{c}_{i\alpha}\hat{c}_{i\beta}, \tag{18c}$$

$$\hat{\rho}(b\hat{T} + \hat{u}^2_\alpha) = \sum_{i=1}^{I} \hat{f}^{\mathrm{eq}}_i(\hat{c}^2_{i\alpha} + \hat{\eta}^2_i), \tag{18d}$$

$$\hat{\rho}[(b+2)\hat{T} + \hat{u}^2_\beta]\hat{u}_\alpha = \sum_{i=1}^{I} \hat{f}^{\mathrm{eq}}_i(\hat{c}^2_{i\beta} + \hat{\eta}^2_i)\hat{c}_{i\alpha}. \tag{18e}$$

We will give a specific model for each number of dimensions D(=1, 2, or 3) that satisfies the above constraints (18a)–(18e).

(1) One-dimensional model ($D=1, I=5$).

Let

$$\hat{c}_{i1} = \begin{cases} 0 & \text{for} \quad i = 1 \\ v_1 \cos(\pi i) & \text{for} \quad i = 2,3 \\ v_2 \cos(\pi i) & \text{for} \quad i = 4,5, \end{cases}$$
$$\hat{\eta}_i = \begin{cases} \eta_0 & \text{for} \quad i = 1 \\ 0 & \text{for} \quad i = 2,3,4,5, \end{cases} \tag{19}$$

where v_1, $v_2(\neq v_1)$, and η_0 are given nonzero constants [see Fig. 1(a)], and let

$$\hat{f}^{\mathrm{eq}}_i = \hat{\rho}(A_i + B_i\hat{u}_1\hat{c}_{i1}) \quad \text{for} \quad i = 1,2,3,4,5 \tag{20}$$

be a local equilibrium velocity distribution function, where

$$A_i = \begin{cases} \dfrac{b-1}{\eta_0^2}\hat{T} & \text{for} \quad i = 1 \\ \dfrac{1}{2(v_1^2 - v_2^2)}\left[-v_2^2 + \left((b-1)\dfrac{v_2^2}{\eta_0^2} + 1\right)\hat{T} + \hat{u}_1^2\right] & \text{for} \quad i = 2,3 \\ \dfrac{1}{2(v_2^2 - v_1^2)}\left[-v_1^2 + \left((b-1)\dfrac{v_1^2}{\eta_0^2} + 1\right)\hat{T} + \hat{u}_1^2\right] & \text{for} \quad i = 4,5, \end{cases} \tag{21a}$$

$$B_i = \begin{cases} \dfrac{-v_2^2 + (b+2)\hat{T} + \hat{u}_1^2}{2v_1^2(v_1^2 - v_2^2)} & \text{for} \quad i = 2,3 \\ \dfrac{-v_1^2 + (b+2)\hat{T} + \hat{u}_1^2}{2v_2^2(v_2^2 - v_1^2)} & \text{for} \quad i = 4,5. \end{cases} \tag{21b}$$

Then $\hat{c}_{i1}$, $\hat{\eta}_i$, and $\hat{f}^{\mathrm{eq}}_i$ ($i=1,2,3,4,5$) given above satisfy the constraints (18a)–(18e). This is the first lattice Boltzmann model of one-dimensional version whose specific-heat ratio γ [which is related to b by Eq. (3)] can be chosen according to our convenience, while the previous model gives the unphysical value of $\gamma=3$ (or $b=1$) only.

(2) Two-dimensional model ($D=2, I=9$).
Let

$$(\hat{c}_{i1},\hat{c}_{i2})=\begin{cases}(0,0) & \text{for} \quad i=1\\ v_1\left(\cos\dfrac{\pi i}{2},\sin\dfrac{\pi i}{2}\right) & \text{for} \quad i=2,3,4,5\\ v_2\left[\cos\ \pi\left(\dfrac{i}{2}+\dfrac{1}{4}\right),\sin\ \pi\left(\dfrac{i}{2}+\dfrac{1}{4}\right)\right] & \text{for} \quad i=6,7,8,9,\end{cases} \qquad \hat{\eta}_i=\begin{cases}\eta_0 & \text{for} \quad i=1\\ 0 & \text{for} \quad i=2,3,\ldots,9,\end{cases} \tag{22}$$

where v_1, $v_2(\neq v_1)$, and η_0 are given nonzero constants [see Fig. 1(b)], and let

$$\hat{f}_i^{\mathrm{eq}}=\hat{\rho}(A_i+B_i\hat{u}_\alpha\hat{c}_{i\alpha}+D_i\hat{u}_\alpha\hat{c}_{i\alpha}\hat{u}_\beta\hat{c}_{i\beta}) \quad \text{for} \quad i=1,2,\ldots,9 \tag{23}$$

be a local equilibrium velocity distribution function, where

$$A_i=\begin{cases}\dfrac{b-2}{\eta_0^2}\hat{T} & \text{for} \quad i=1\\ \dfrac{1}{4(v_1^2-v_2^2)}\left[-v_2^2+\left((b-2)\dfrac{v_2^2}{\eta_0^2}+2\right)\hat{T}+\dfrac{v_2^2}{v_1^2}\hat{u}_\alpha^2\right] & \text{for} \quad i=2,3,4,5\\ \dfrac{1}{4(v_2^2-v_1^2)}\left[-v_1^2+\left((b-2)\dfrac{v_1^2}{\eta_0^2}+2\right)\hat{T}+\dfrac{v_1^2}{v_2^2}\hat{u}_\alpha^2\right] & \text{for} \quad i=6,7,8,9,\end{cases} \tag{24a}$$

$$B_i=\begin{cases}\dfrac{-v_2^2+(b+2)\hat{T}+\hat{u}_\beta^2}{2v_1^2(v_1^2-v_2^2)} & \text{for} \quad i=2,3,4,5\\ \dfrac{-v_1^2+(b+2)\hat{T}+\hat{u}_\beta^2}{2v_2^2(v_2^2-v_1^2)} & \text{for} \quad i=6,7,8,9,\end{cases} \tag{24b}$$

$$D_i=\begin{cases}\dfrac{1}{2v_1^4} & \text{for} \quad i=2,3,4,5\\ \dfrac{1}{2v_2^4} & \text{for} \quad i=6,7,8,9.\end{cases} \tag{24c}$$

Then $\hat{c}_{i\alpha}$ $(\alpha=1,2)$, $\hat{\eta}_i$, and $\hat{f}_i^{\mathrm{eq}}$ $(i=1,2,\ldots,9)$ given above satisfy the constraints (18a)–(18e). Compared with the previously proposed model [1], this model is superior in the computational efficiency, since the number of molecular velocities is reduced from 17 to 9. Thus, the computation time is almost halved.

(3) Three-dimensional model ($D=3$, $I=15$).
Let

$$(\hat{c}_{i1},\hat{c}_{i2},\hat{c}_{i3})=\begin{cases}(0,0,0) & \text{for} \quad i=1\\ v_1(\pm1,0,0),\ v_1(0,\pm1,0),\ v_1(0,0,\pm1) & \text{for} \quad i=2,3,\ldots,7\\ \dfrac{v_2}{\sqrt{3}}(\pm1,\pm1,\pm1) & \text{for} \quad i=8,9,\ldots,15,\end{cases} \qquad \hat{\eta}_i=\begin{cases}\eta_0 & \text{for} \quad i=1\\ 0 & \text{for} \quad i=2,3,\ldots,15,\end{cases} \tag{25}$$

where v_1, $v_2(\neq v_1)$, and η_0 are given nonzero constants [see Fig. 1(c)], and let

$$\hat{f}_i^{\mathrm{eq}}=\hat{\rho}(A_i+B_i\hat{u}_\alpha\hat{c}_{i\alpha}+D_i\hat{u}_\alpha\hat{c}_{i\alpha}\hat{u}_\beta\hat{c}_{i\beta}) \quad \text{for} \quad i=1,2,\ldots,15 \tag{26}$$

be a local equilibrium velocity distribution function, where

$$A_i = \begin{cases} \dfrac{b-3}{\eta_0^2}\hat{T} & \text{for} \quad i=1 \\ \dfrac{1}{6(v_1^2-v_2^2)}\left[-v_2^2+\left((b-3)\dfrac{v_2^2}{\eta_0^2}+3\right)\hat{T}+\dfrac{v_2^2}{v_1^2}\hat{u}_\alpha^2\right] & \text{for} \quad i=2,3,\ldots,7 \\ \dfrac{1}{8(v_2^2-v_1^2)}\left[-v_1^2+\left((b-3)\dfrac{v_1^2}{\eta_0^2}+3\right)\hat{T}+\dfrac{3v_1^2-v_2^2}{2v_2^2}\hat{u}_\alpha^2\right] & \text{for} \quad i=8,9,\ldots,15, \end{cases} \tag{27a}$$

$$B_i = \begin{cases} \dfrac{-v_2^2+(b+2)\hat{T}+\hat{u}_\beta^2}{2v_1^2(v_1^2-v_2^2)} & \text{for} \quad i=2,3,\ldots,7 \\ \dfrac{3\left[-v_1^2+(b+2)\hat{T}+\hat{u}_\beta^2\right]}{8v_2^2(v_2^2-v_1^2)} & \text{for} \quad i=8,9,\ldots,15, \end{cases} \tag{27b}$$

$$D_i = \begin{cases} \dfrac{1}{2v_1^4} & \text{for} \quad i=2,3,\ldots,7 \\ \dfrac{9}{16v_2^4} & \text{for} \quad i=8,9,\ldots,15. \end{cases} \tag{27c}$$

Then $\hat{c}_{i\alpha}$ $(\alpha=1,2,3)$, $\hat{\eta}_i$, and $\hat{f}_i^{\mathrm{eq}}$ $(i=1,2,\ldots,15)$ given above satisfy the constraints (18a)–(18e). This is the first lattice Boltzmann model of three-dimensional version whose specific-heat ratio can be chosen according to our convenience.

III. ASYMPTOTIC ANALYSIS

In this section the asymptotic analysis for small ε of the initial-value problem (15) and (16) is carried out to investigate the behavior of a solution in the limit of $\varepsilon \to 0$. We consider the case where the deviation of $\hat{f}_i$ from that of a uniform reference state at rest is of the order of unity (or the Mach number of the flow is of the order of unity) throughout. When the scale of variation is of the order of unity with respect to $\hat{t}$ and $\hat{x}_\alpha$, the usual asymptotic analysis [16,17] is applied. This is explained in Sec. III A. We will find that the macroscopic variables obtained from the kinetic equation (15) with the initial condition (16) satisfy, in the limit of $\varepsilon \to 0$, the compressible Euler equations (11a)–(11c) and their initial condition (13).

In contrast, when the shock waves and contact discontinuities appear and the solution includes the regions of steep variation, the effect of steep variation must be taken into account correctly in the analysis. This case is treated in Sec. III B. Since the usual finite-difference scheme of the kinetic equation (15) of the mesh width $O(\varepsilon)$ is not consistent with the kinetic equation itself (see Sec. I), but with the integral relation (see Appendix), the integral relation of the kinetic equation is used as a basic equation. Then the macroscopic variables obtained from the integral relation are found to satisfy, in the limit of $\varepsilon \to 0$, the weak form of the Euler equations.

The following analysis is based on the general model, Eqs. (15)–(18), and application to the concrete models is straightforward: only to substitute $\hat{c}_{i\alpha}$, $\hat{\eta}_i$, and $\hat{f}_i^{\mathrm{eq}}$ of the specific model given by Eqs. (19) and (20), or (22) and (23) or (25) and (26), into the corresponding parts of the following analysis. For the sake of clarity, a proposition is suggested first and its proof is given subsequently.

A. Solutions of moderate variation

Proposition 1. Consider a case where the solution $\hat{f}_i$ makes an appreciable variation over $\hat{t}$ and $\hat{x}_\alpha$ of the order of unity at any place. Then the solution $\hat{f}_i$ of the initial-value problem, Eqs. (15) and (16), in the limit of $\varepsilon \to 0$ is given by $\hat{f}_i = \hat{f}_i^{\mathrm{eq}}(\hat{\rho}, \hat{u}, \hat{T})$ whose macroscopic variables $\hat{\rho}$, $\hat{u}$, and $\hat{T}$ satisfy the compressible Euler equations (11a)–(11c) and their initial condition (13).

Proof. We look for the asymptotic solution of Eq. (15) for small ε whose scale of variation is of the order of unity with respect to the coordinates $\hat{t}$ and $\hat{x}_\alpha$, in a power series of ε [22]:

$$\hat{f}_i = \hat{f}_i^{(0)} + \varepsilon \hat{f}_i^{(1)} + \varepsilon^2 \hat{f}_i^{(2)} + \cdots, \tag{28}$$

where the component function $\hat{f}_i^{(m)}$ $(m=0,1,2,\ldots)$ is a quantity of the order of unity.

Macroscopic variables are also expanded:

$$\hat{h} = \hat{h}^{(0)} + \varepsilon \hat{h}^{(1)} + \varepsilon^2 \hat{h}^{(2)} + \cdots, \tag{29}$$

where $\hat{h}$ represents any of the macroscopic variables $\hat{\rho}$, $\hat{u}_\alpha$, $\hat{T}$, and $\hat{p}$. The component functions $\hat{h}^{(m)}$ satisfy the relations derived from Eqs. (14a)–(14c) and (12). Only the leading-order relations are explicitly given:

$$\hat{\rho}^{(0)} = \sum_{i=1}^{I} \hat{f}_i^{(0)}, \tag{30a}$$

$$\hat{\rho}^{(0)}\hat{u}_\alpha^{(0)} = \sum_{i=1}^{I} \hat{f}_i^{(0)}\hat{c}_{i\alpha}, \tag{30b}$$

$$\hat{\rho}^{(0)}[b\hat{T}^{(0)} + (\hat{u}_\alpha^{(0)})^2] = \sum_{i=1}^{I} \hat{f}_i^{(0)}(\hat{c}_{i\alpha}^2 + \hat{\eta}_i^2), \tag{30c}$$

$$\hat{p}^{(0)} = \hat{\rho}^{(0)}\hat{T}^{(0)}. \tag{30d}$$

The equilibrium distribution function is also expanded as follows:

$$\hat{f}_i^{\mathrm{eq}} = \hat{f}_i^{\mathrm{eq}(0)} + \varepsilon \hat{f}_i^{\mathrm{eq}(1)} + \varepsilon^2 \hat{f}_i^{\mathrm{eq}(2)} + \cdots. \tag{31}$$

The component function $\hat{f}_i^{\mathrm{eq}(m)}$ satisfies the following constraints from Eqs. (18a)–(18e):

$$\hat{\rho}^{(0)} = \sum_{i=1}^{I} \hat{f}_i^{\mathrm{eq}(0)}, \tag{32a}$$

$$\hat{\rho}^{(0)}\hat{u}_\alpha^{(0)} = \sum_{i=1}^{I} \hat{f}_i^{\mathrm{eq}(0)}\hat{c}_{i\alpha}, \tag{32b}$$

$$\hat{p}^{(0)}\delta_{\alpha\beta} + \hat{\rho}^{(0)}\hat{u}_\alpha^{(0)}\hat{u}_\beta^{(0)} = \sum_{i=1}^{I} \hat{f}_i^{\mathrm{eq}(0)}\hat{c}_{i\alpha}\hat{c}_{i\beta}, \tag{32c}$$

$$\hat{\rho}^{(0)}[b\hat{T}^{(0)} + (\hat{u}_\alpha^{(0)})^2] = \sum_{i=1}^{I} \hat{f}_i^{\mathrm{eq}(0)}(\hat{c}_{i\alpha}^2 + \hat{\eta}_i^2), \tag{32d}$$

$$\hat{\rho}^{(0)}[(b+2)\hat{T}^{(0)} + (\hat{u}_\beta^{(0)})^2]\hat{u}_\alpha^{(0)} = \sum_{i=1}^{I} \hat{f}_i^{\mathrm{eq}(0)}(\hat{c}_{i\beta}^2 + \hat{\eta}_i^2)\hat{c}_{i\alpha}, \tag{32e}$$

$$\cdots.$$

where only the leading-order constraints are explicitly given.

Substituting Eqs. (28) and (31) into Eq. (15) and arranging the same order terms in ε, we obtain the following series of equations for $\hat{f}_i^{(m)}$:

$$\hat{f}_i^{\mathrm{eq}(0)} - \hat{f}_i^{(0)} = 0, \tag{33a}$$

$$\hat{f}_i^{\mathrm{eq}(1)} - \hat{f}_i^{(1)} = \frac{\partial \hat{f}_i^{(0)}}{\partial \hat{t}} + \hat{c}_{i\beta}\frac{\partial \hat{f}_i^{(0)}}{\partial \hat{x}_\beta}, \tag{33b}$$

$$\cdots.$$

The solution of Eq. (33a) is

$$\hat{f}_i^{(0)} = \hat{f}_i^{\mathrm{eq}(0)}(\hat{\rho}^{(0)}, \hat{u}_\alpha^{(0)}, \hat{T}^{(0)}). \tag{34}$$

Equation (33b) for $\hat{f}_i^{(1)}$ is linear and inhomogeneous. From the relation $\Sigma_{i=1}^{i=I} g_i(\hat{f}_i^{\mathrm{eq}(1)} - \hat{f}_i^{(1)}) = 0$, where

$$g_i = 1, \quad \hat{c}_{i\alpha}, \quad \text{or} \quad \hat{c}_{i\alpha}^2 + \hat{\eta}_i^2, \tag{35}$$

Eq. (33b) has a solution only when its inhomogeneous term satisfies the following relation (solvability condition):

$$\sum_{i=1}^{I} g_i\left(\frac{\partial \hat{f}_i^{(0)}}{\partial \hat{t}} + \hat{c}_{i\beta}\frac{\partial \hat{f}_i^{(0)}}{\partial \hat{x}_\beta}\right) = 0. \tag{36}$$

When condition (36) is satisfied, the solution of Eq. (33b) is given by

$$\hat{f}_i^{(1)} = \hat{f}_i^{\mathrm{eq}(1)} - \frac{\partial \hat{f}_i^{(0)}}{\partial \hat{t}} - \hat{c}_{i\beta}\frac{\partial \hat{f}_i^{(0)}}{\partial \hat{x}_\beta}. \tag{37}$$

Substituting Eq. (34) into the solvability condition (36), we can get the equations for the leading-order component functions of the macroscopic variables:

$$\frac{\partial \hat{\rho}^{(0)}}{\partial \hat{t}} + \frac{\partial \hat{\rho}^{(0)}\hat{u}_\alpha^{(0)}}{\partial \hat{x}_\alpha} = 0, \tag{38a}$$

$$\frac{\partial \hat{\rho}^{(0)}\hat{u}_\alpha^{(0)}}{\partial \hat{t}} + \frac{\partial \hat{\rho}^{(0)}\hat{u}_\alpha^{(0)}\hat{u}_\beta^{(0)}}{\partial \hat{x}_\beta} + \frac{\partial \hat{p}^{(0)}}{\partial \hat{x}_\alpha} = 0, \tag{38b}$$

$$\frac{\partial \hat{\rho}^{(0)}[b\hat{T}^{(0)} + (\hat{u}_\alpha^{(0)})^2]}{\partial \hat{t}} + \frac{\partial \hat{\rho}^{(0)}\hat{u}_\alpha^{(0)}[b\hat{T}^{(0)} + (\hat{u}_\beta^{(0)})^2] + 2\hat{p}^{(0)}\hat{u}_\alpha^{(0)}}{\partial \hat{x}_\alpha} = 0, \tag{38c}$$

where Eqs. (32a)–(32e) are used. We can proceed with the analysis to the higher orders in a similar way. One finds that the leading-order set (38a)–(38c) corresponds with the compressible Euler set of equations (11a)–(11c). However, the next-order set, which is not explicitly given here, includes terms that never arise in the Euler equations, and will contribute to the error of the LBM.

As for the initial condition of the leading-order set (38a)–(38c), it is given by the leading-order macroscopic variables $\hat{\rho}^{(0)}, \hat{u}_\alpha^{(0)}, \hat{T}^{(0)}$ in the limit of $\hat{t} \to 0+$. According to Eq. (34), the leading-order velocity distribution function is given by $\hat{f}_i^{(0)} = \hat{f}_i^{\mathrm{eq}(0)}(\hat{\rho}^{(0)}, \hat{u}_\alpha^{(0)}, \hat{T}^{(0)})$, and this fits to the initial condition [Eq. (16)] by setting its macroscopic variables $\hat{\rho}^{(0)} = \hat{\rho}^0$, $\hat{u}_\alpha^{(0)} = \hat{u}_\alpha^0$, and $\hat{T}^{(0)} = \hat{T}^0$. Thus, the initial condition for the leading-order set (38a)–(38c) is given by $\hat{\rho}^{(0)} = \hat{\rho}^0$, $\hat{u}_\alpha^{(0)} = \hat{u}_\alpha^0$, and $\hat{T}^{(0)} = \hat{T}^0$.

Thus, the solution $\hat{f}_i$ of the initial-value problem (15) and (16) in the limit of $\varepsilon \to 0$ is given by the local equilibrium distribution function, or Eq. (34), and its macroscopic variables satisfy the compressible Euler equations (11a)–(11c) and their initial condition (13). ■

B. Solutions with steep variation

In order to make a discussion simple, we consider the one-dimensional problem in this section. The subscripts α and β representing the spatial directions are omitted. The extension of the discussion in this section to the two or three-dimensional problems is straightforward.

It is well known that flows with shock waves and contact discontinuities can be correctly described by the weak solutions of the compressible Euler equations with the subsidiary entropy condition [13–15]. The weak solutions of the initial-value problem of the Euler equations (11a)–(11c) with Eq. (13) are the solutions of the following integral relation:

$$\int_{-\infty}^{\infty} d\hat{x} \int_{0}^{\infty} \left(\frac{\partial \psi}{\partial \hat{t}} \begin{Bmatrix} \hat{\rho} \\ \hat{\rho}\hat{u} \\ \hat{\rho}(b\hat{T} + \hat{u}^2) \end{Bmatrix} + \frac{\partial \psi}{\partial \hat{x}} \begin{Bmatrix} \hat{\rho}\hat{u} \\ \hat{\rho}\hat{u}^2 + \hat{p} \\ \hat{\rho}\hat{u}(b\hat{T} + \hat{u}^2) + 2\hat{p}\hat{u} \end{Bmatrix} \right) d\hat{t} + \int_{-\infty}^{\infty} \begin{Bmatrix} \hat{\rho}^0 \\ \hat{\rho}^0\hat{u}^0 \\ \hat{\rho}^0[b\hat{T}^0 + (\hat{u}^0)^2] \end{Bmatrix} \psi(0,\hat{x}) d\hat{x} = 0, \tag{39}$$

where $\psi(\hat{t},\hat{x})$ is any smooth test function of $\hat{t}$ and $\hat{x}$, which vanishes for $\hat{t}+|\hat{x}|$ large enough. The integral relation (39) is called the weak form of the Euler equations. According to Refs. [13–15], the solutions of the integral relation (39) satisfy the Euler equations themselves in the regions where the solution is smooth, and they satisfy, at their discontinuities, the correct jump conditions derived from the conservation form of the compressible Euler equations (or the Rankine-Hugoniot relations [10,23]).

In order to obtain the weak solutions of the Euler equations, or the solutions of the integral relation (39) by the kinetic-equation system, we consider the following integral relation derived from the kinetic equation (15) and the initial condition (16):

$$\int_{-\infty}^{\infty} d\hat{x} \int_{0}^{\infty} \left[\left(\frac{\partial \psi}{\partial \hat{t}} + \hat{c}_i \frac{\partial \psi}{\partial \hat{x}} \right) \hat{f}_i + \frac{\hat{f}_i^{\mathrm{eq}}(\hat{\rho},\hat{u},\hat{T}) - \hat{f}_i}{\varepsilon} \psi \right] d\hat{t} + \int_{-\infty}^{\infty} \hat{f}_i^{\mathrm{eq}}(\hat{\rho}^0,\hat{u}^0,\hat{T}^0) \psi(0,\hat{x}) d\hat{x} = 0, \tag{40}$$

where ψ is the above-mentioned test function which is independent of ε. The finite-difference scheme of Eq. (15) is consistent with this integral relation (40) even if the mesh width is $O(\varepsilon)$ (see the Appendix for proof). Therefore we make an analysis on the basis of Eq. (40). According to the analysis of the Boltzmann equation, shock waves and contact discontinuities are not real discontinuities but the thin layers of width $O(\varepsilon)$ across which the variables make an appreciable variation. In view of these facts, assuming the similar situation, we suggest the following proposition.

Proposition 2. Consider a case where the solution $\hat{f}_i$ makes steep variation in several localized regions representing, for example, shock waves and contact discontinuities. In the regions, the solution $\hat{f}_i$ makes an appreciable variation over $\hat{t}$ and $\hat{x}$ of $O(\varepsilon)$. In the other regions, which are called the Euler regions, it makes a moderate variation (an appreciable variation over $\hat{t}$ and $\hat{x}$ of order unity). Then the solution $\hat{f}_i$ of Eq. (40) in the limit of $\varepsilon \to 0$ is given by $\hat{f}_i = \hat{f}_i^{\mathrm{eq}}(\hat{\rho},\hat{u},\hat{T})$ whose macroscopic variables $\hat{\rho}$, $\hat{u}$, and $\hat{T}$ satisfy the integral relation (39), or the weak form of the compressible Euler equations.

Proof. The localized regions of steep variation are represented by several thin layers of width $O(\varepsilon)$ on the $\hat{t}-\hat{x}$ plane. The variables inside these layers are attached with the subscript S, i.e., $\hat{f}_{iS}$, $\hat{f}_{iS}^{\mathrm{eq}}$, and $\hat{h}_S$ ($\hat{h}$ represents any of the macroscopic variables). Their scale of variation is of the order of unity in the direction along the layers, and of the order of ε normal to the layers. The variables in the Euler regions are attached with the subscript E, i.e., $\hat{f}_{iE}$, $\hat{f}_{iE}^{\mathrm{eq}}$, and $\hat{h}_E$. Their scale of variation is of the order of unity but have discontinuities across the thin layers of steep variation. The variables in the thin layers (with the subscript S) converge to those in the Euler regions (with the subscript E) very rapidly as the distance normal to the layers increases.

In order to make the asymptotic analysis for small ε, we expand the variables in power series of ε like Eqs. (28), (29), and (31) with the subscript E or S attached to each variable. The component functions have the magnitude of order of unity and they satisfy the same relations as Eqs. (30a)–(30d) and (32a)–(32e), where the subscripts α and β are removed and E or S is attached to each variable.

Substituting the expanded series of variables into Eq. (40) and noting that the integral area of the layers of steep variation with nonzero value of ψ is $O(\varepsilon)$, we arrange the same order terms in ε. We then obtain the following series of integral relations:

$$\int_{-\infty}^{\infty} d\hat{x} \int_{0}^{\infty} (\hat{f}_{iE}^{(0)} - \hat{f}_{iE}^{\mathrm{eq}(0)}) \psi d\hat{t} = 0, \tag{41a}$$

$$\int_{-\infty}^{\infty} d\hat{x} \int_{0}^{\infty} \left[\left(\frac{\partial \psi}{\partial \hat{t}} + \hat{c}_i \frac{\partial \psi}{\partial \hat{x}} \right) \hat{f}_{iE}^{(0)} + (\hat{f}_{iE}^{(1)} - \hat{f}_{iE}^{\mathrm{eq}(1)}) \psi \right] d\hat{t} + \int_{-\infty}^{\infty} \hat{f}_{iE}^{\mathrm{eq}(0)}(\hat{\rho}^0,\hat{u}^0,\hat{T}^0) \psi(0,\hat{x}) d\hat{x} + \int\int_{D_s} [(\hat{f}_{iS}^{(0)} - \hat{f}_{iS}^{\mathrm{eq}(0)}) - (\hat{f}_{iE}^{(0)} - \hat{f}_{iE}^{\mathrm{eq}(0)})] \psi d\hat{t} d\hat{x} = 0, \tag{41b}$$

where D_S indicates the domain of steep variation on the $\hat{t}-\hat{x}$ plane.

From the leading-order relation (41a), we get

$$\hat{f}_{iE}^{(0)} = \hat{f}_{iE}^{\mathrm{eq}(0)}(\hat{\rho}_E^{(0)},\hat{u}_E^{(0)},\hat{T}_E^{(0)}), \tag{42}$$

since ψ is arbitrary.

The next-order equation (41b) can be seen as a linear inhomogeneous equation for $\hat{f}_{iE}^{(1)}$. From the relation $\Sigma_{i=1}^{i=I} g_i(\hat{f}_{iE}^{\mathrm{eq}(1)} - \hat{f}_{iE}^{(1)}) = 0$, where g_i is given by Eq. (35), Eq. (41b) has a solution only when its inhomogeneous term satisfies the following relation (solvability condition):

$$\sum_{i=1}^{I} g_i \left\{ \int_{-\infty}^{\infty} d\hat{x} \int_0^{\infty} \left(\frac{\partial \psi}{\partial \hat{t}} + \hat{c}_i \frac{\partial \psi}{\partial \hat{x}} \right) \hat{f}_{iE}^{(0)} d\hat{t} + \int_{-\infty}^{\infty} \hat{f}_{iE}^{\mathrm{eq}(0)}(\hat{\rho}^0, \hat{u}^0, \hat{T}^0) \psi(0,\hat{x}) d\hat{x} + \int\int_{D_s} [(\hat{f}_{iS}^{(0)} - \hat{f}_{iS}^{\mathrm{eq}(0)}) - (\hat{f}_{iE}^{(0)} - \hat{f}_{iE}^{\mathrm{eq}(0)})] \psi d\hat{t} d\hat{x} \right\} = 0. \tag{43}$$

Substituting Eq. (42) into the solvability condition (43), we get the following integral relation for the leading-order component functions of the macroscopic variables in the Euler regions $\hat{\rho}_E^{(0)}$, $\hat{u}_E^{(0)}$, $\hat{T}_E^{(0)}$, and $\hat{p}_E^{(0)}$:

$$\int_{-\infty}^{\infty} d\hat{x} \int_0^{\infty} \left(\frac{\partial \psi}{\partial \hat{t}} \begin{Bmatrix} \hat{\rho}_E^{(0)} \\ \hat{\rho}_E^{(0)} \hat{u}_E^{(0)} \\ \hat{\rho}_E^{(0)} (b\hat{T}_E^{(0)} + (\hat{u}_E^{(0)})^2) \end{Bmatrix} + \frac{\partial \psi}{\partial \hat{x}} \begin{Bmatrix} \hat{\rho}_E^{(0)} \hat{u}_E^{(0)} \\ \hat{\rho}_E^{(0)} (\hat{u}_E^{(0)})^2 + \hat{p}_E^{(0)} \\ \hat{\rho}_E^{(0)} \hat{u}_E^{(0)} (b\hat{T}_E^{(0)} + (\hat{u}_E^{(0)})^2) + 2\hat{p}_E^{(0)} \hat{u}_E^{(0)} \end{Bmatrix} \right) d\hat{t} + \int_{-\infty}^{\infty} \begin{Bmatrix} \hat{\rho}^0 \\ \hat{\rho}^0 \hat{u}^0 \\ \hat{\rho}^0 (b\hat{T}^0 + (\hat{u}^0)^2) \end{Bmatrix} \psi(0,\hat{x}) d\hat{x} = 0, \tag{44}$$

where Eqs. (32a)–(32e) (with the subscripts α, β removed and E attached to each variable) and $\Sigma_{i=1}^{i=I} g_i(\hat{f}_{iS}^{\mathrm{eq}(0)} - \hat{f}_{iS}^{(0)}) = \Sigma_{i=1}^{i=I} g_i(\hat{f}_{iE}^{\mathrm{eq}(0)} - \hat{f}_{iE}^{(0)}) = 0$ are used. We find that Eq. (44) corresponds with the weak form of the Euler equations (39).

Thus, the solution $\hat{f}_i$ of Eq. (40) in the limit of $\varepsilon \to 0$ is given by the local equilibrium distribution function, or Eq. (42), and its macroscopic variables satisfy the weak form of the compressible Euler equations (39). ■

IV. NUMERICAL EXAMPLES AND ERROR ESTIMATES

Now we present several numerical examples of the lattice Boltzmann models introduced in Sec. II and estimate their errors. The parameters included in Eqs. (19), (22), and (25) are chosen to be $v_1 = 1$, $v_2 = 3$, $\eta_0 = 2$, and the finite-difference scheme with the usual first-order forward in time and the second-order upwind in space is used for the numerical computation of the kinetic equation (15). The mesh width for $\hat{t}$ is set at $\Delta\hat{t} = \varepsilon/4$. The scheme is consistent with the integral relation (40) when computing flows with shocks and contact discontinuities. The consistency is shown in Appendix. Note that the entropy condition is not guaranteed to be satisfied by the scheme, since it cannot realize the internal structure of the shock waves. Thus, the shock waves across which the entropy of fluid particles decreases may appear in the numerical results. However, we believe that such shocks will practically not appear. This estimate will be demonstrated in Sec. IV B, where only the shocks across which the entropy of fluid particles increases are found to appear in all the numerical results.

A. Propagation of expansion waves

We consider the one-dimensional initial-value problem of Eqs. (15) and (16) with $D = 1$ whose initial macroscopic variables are given by

$$\hat{\rho}^0 = \hat{T}^0 = 1, \quad \hat{u}_1^0 = U \tanh \hat{x}_1, \tag{45}$$

where U is a given constant. It is expected that, when $U > 0$, only the expansion waves will propagate and no shock waves will appear. This problem is characterized by the three parameters ε, U, and γ (or b).

The numerical results (flow velocity, pressure, density, and temperature) at $\hat{t} = 1$ with $\varepsilon = 10^{-4}$ and $U = 1$ are shown for three different values of $\gamma = 5/3$, $7/5$, and $9/7$ (or $b = 3$, 5, and 7) in Fig. 2 by the plots. The one-dimensional lattice Boltzmann model, Eqs. (19), (20), (21a), and (21b), was used for calculation. The corresponding numerical results of the Euler equations themselves solved by the so-called MacCormack scheme [24] with sufficient number of meshes are shown by the lines. We find a good agreement between the two results for each value of γ.

The error of the LBM is now defined as

$$E = \int_{-\infty}^{\infty} |\hat{u}_1 - \hat{u}_1^{\mathrm{exa}}| d\hat{x}_1, \tag{46}$$

where the variable with the superscript 'exa' represents the exact solution. Here we used the numerical solution by the MacCormack method with sufficient number of meshes as the exact solution. In Fig. 3, E is plotted as a function of the spatial mesh width $\Delta\hat{x}$. One finds that E is proportional to $(\Delta\hat{x})^2$ when $\Delta\hat{x}$ is relatively large, since the second-order finite-difference scheme is used. For the smaller value of $\Delta\hat{x}$, however, we find that E asymptotes to some value that is proportional to ε. This is the error inherent to the LBM, since the macroscopic variables obtained from the solution of the LBM satisfy the Euler equations at the leading order [or $O(1)$] but not at the next order [or $O(\varepsilon)$] as mentioned in Sec. III A [see the statements below Eqs. (38a)–(38c)]. Thus, the result of the asymptotic analysis in Sec. III A has been supported numerically.

B. Riemann problem

In this section we focus our attention on flows with steep variation, or the Riemann problem: the initial-value problem of the one-dimensional integral relation (40) whose initial macroscopic variables $\hat{\rho}^0$, $\hat{u}^0$, and $\hat{T}^0$ are piecewise constant, with one jump discontinuity. Note that the Riemann problem has no characteristic length in the initial condition so that the

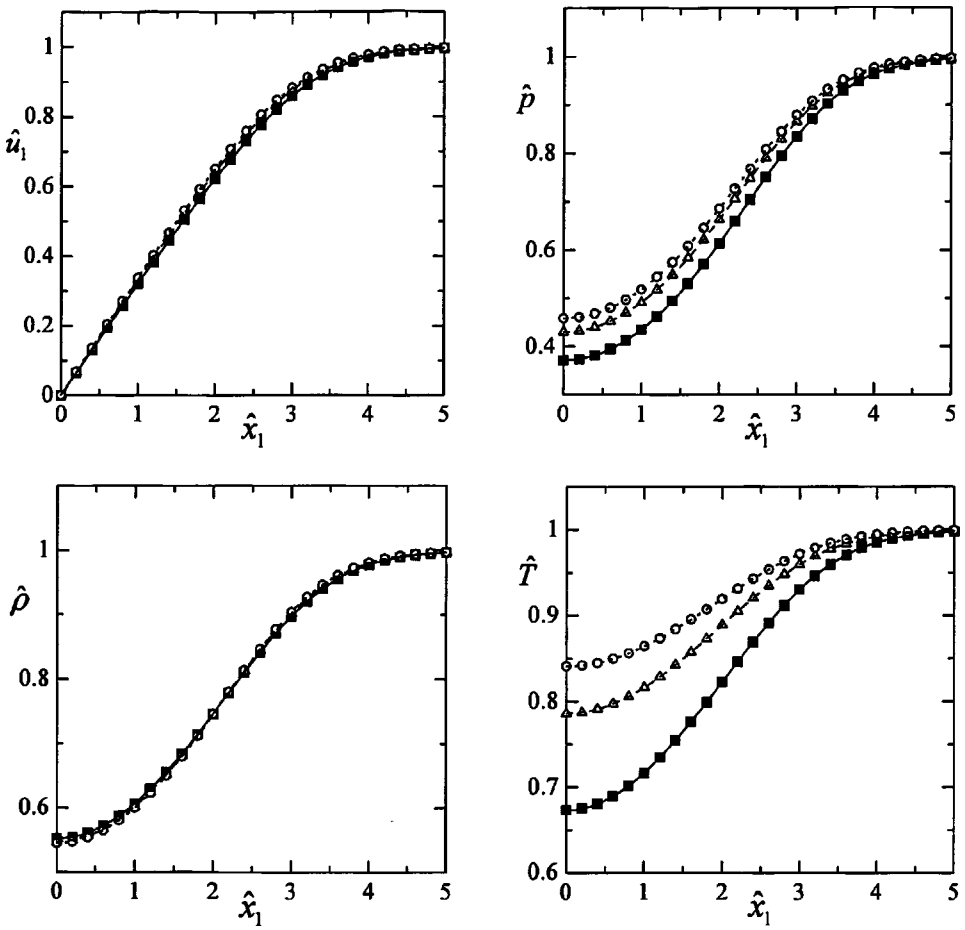

FIG. 2. The $\hat{x}_1$ dependence of $\hat{u}_1$, $\hat{p}$, $\hat{\rho}$, and $\hat{T}$ at $\hat{t}=1$ of the numerical results for the one-dimensional problem whose initial condition is Eq. (45) with $\varepsilon=10^{-4}$ and $U=1$. The plots are the results by the LBM with $\Delta\hat{x}=0.02$: ■, $\gamma=5/3$; △, $\gamma=7/5$; ◯, $\gamma=9/7$. The lines represent the corresponding results by the Mac-Cormack method with sufficient number of meshes: $\gamma=5/3$ (solid lines), 7/5 (dashed lines), and 9/7 (dotted lines). From the symmetry of the problem with respect to $\hat{x}_1=0$, only the results for $\hat{x}_1>0$ are shown.

time of our interest is chosen as the characteristic time t_0. Thus, the nondimensinal times $\hat{t}$ of the following results are always 1, and the characteristic length becomes $\sqrt{RT_0}\,t_0$.

First, consider the one-dimensional initial-value problem of Eq. (40) whose initial macroscopic variables are given by

$$\hat{\rho}^0=\hat{T}^0=1, \quad \hat{u}_1^0=\begin{cases} U & \text{for} \quad \hat{x}_1<0 \\ -U & \text{for} \quad \hat{x}_1>0, \end{cases} \tag{47}$$

where U is a given constant. This problem is characterized by the three parameters ε, U, and γ (or b).

The numerical results with $\varepsilon=10^{-4}$ and $U=1$ are shown for three different values of $\gamma=5/3$, 7/5, and 9/7 (or $b=3$, 5, and 7) in Fig. 4 by the plots. The one-dimensional lattice Boltzmann model, Eqs. (19), (20), (21a), and (21b), was used for calculation. The corresponding exact theoretical solutions [25] are shown by the lines. We find a good agreement between the two results for each value of γ. Some numerical data that are far below the exact solution adjacent to the shock, are only due to the use of numerical scheme whose mesh width is $O(\varepsilon)$ that could incur the error of order unity in the shock region only.

The error E defined by Eq. (46), with $\hat{u}_1^{\mathrm{exa}}$ given by the exact theoretical solution, is plotted as a function of $\Delta\hat{x}$ in Fig. 5. One finds that E is proportional to $\Delta\hat{x}$ for relatively large $\Delta\hat{x}$, although the second-order finite-difference scheme is used. This error is a contribution from the shock layer inside which the error of the solution is of the order of unity, and the width of the layer is proportional to $\Delta\hat{x}$. For the smaller value of $\Delta\hat{x}$, however, E asymptotes to some value that is proportional to ε, since the width of the shock layer asymptotes to the value proportional to ε.

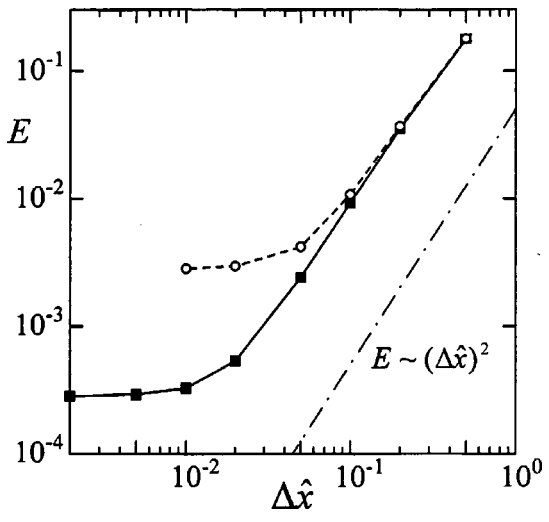

FIG. 3. The $\Delta\hat{x}$ dependence of E for the numerical results of the one-dimensional problem whose initial condition is given by Eq. (45) with $U=1$ and $\gamma=5/3$, ◯,, $\varepsilon=10^{-3}$; ■, $\varepsilon=10^{-4}$. The dash-dot line in the figure represents $E\sim\Delta\hat{x}^2$.

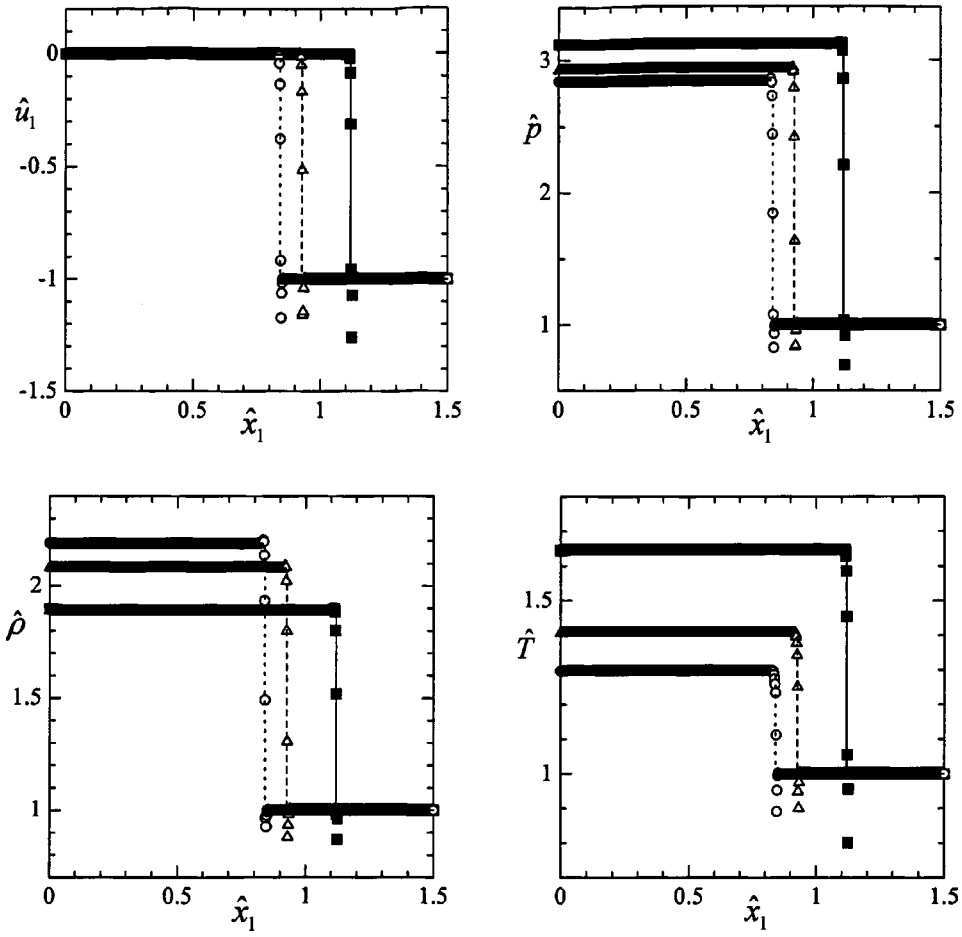

FIG. 4. The $\hat{x}_1$ dependence of $\hat{u}_1$, $\hat{p}$, $\hat{\rho}$, and $\hat{T}$ of the results by the LBM for the one-dimensional problem whose initial condition is Eq. (47) with $\varepsilon=10^{-4}$ and $U=1$. The plots are the results by the LBM with $\Delta\hat{x}=0.002$: ■, $\gamma=5/3$; △, $\gamma=7/5$; ◯, $\gamma=9/7$. The lines represent the corresponding theoretical solutions for $\gamma=5/3$ (solid lines), 7/5 (dashed lines), and 9/7 (dotted lines). From the symmetry of the problem with respect to $\hat{x}_1=0$, only the results for $\hat{x}_1>0$ are shown.

Next, we consider the shock-tube problem. The initial macroscopic variables are given by

$$\hat{p}^0=\begin{cases}1 & \text{for} \quad \hat{x}_1<0\\ P & \text{for} \quad \hat{x}_1>0,\end{cases} \qquad \hat{u}_1^0=0, \quad \hat{T}^0=1, \tag{48}$$

where $\hat{p}^0=\hat{\rho}^0\hat{T}^0$ is the nondimensional initial pressure and P is a given constant. This problem is characterized by the three parameters ε, P, and γ. The numerical results for $\varepsilon=10^{-4}$, $P=5$, and $\gamma=5/3$, 7/5, 9/7 are shown in Fig. 6 by the plots together with the corresponding exact theoretical solutions (represented by the lines). We find a good agreement between the two results for each value of γ. The error E defined by Eq. (46) is plotted in Fig. 7. In this case also, E is proportional to $\Delta\hat{x}$ for relatively large $\Delta\hat{x}$, and E asymptotes to some value that is proportional to ε as $\Delta\hat{x}$ becomes smaller.

From the above numerical examples, we find that flows with steep variation can be described by the finite-difference scheme of Eq. (15) with the error of $O(\varepsilon)+O(\Delta\hat{x})$. By choosing $\Delta\hat{x}\sim\varepsilon$, then, the error becomes $O(\varepsilon)$, and agrees with the result of the asymptotic analysis in Sec. III B.

Finally, we note the following three points. First, we calculated the Riemann problem using the two-and three-dimensional lattice Boltzmann models also. The results gave the same tendency as those of the one-dimensional model presented above. Second, there appeared no shock waves

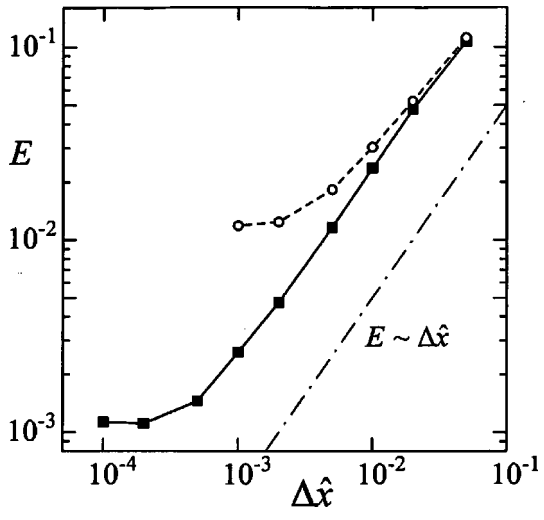

FIG. 5. The $\Delta\hat{x}$ dependence of E for the numerical results of the one-dimensional problem whose initial condition is given by Eq. (47) with $U=1$ and $\gamma=5/3$: ◯, $\varepsilon=10^{-3}$; ■, $\varepsilon=10^{-4}$. The dash-dot line in the figure represents $E\sim\Delta\hat{x}$.

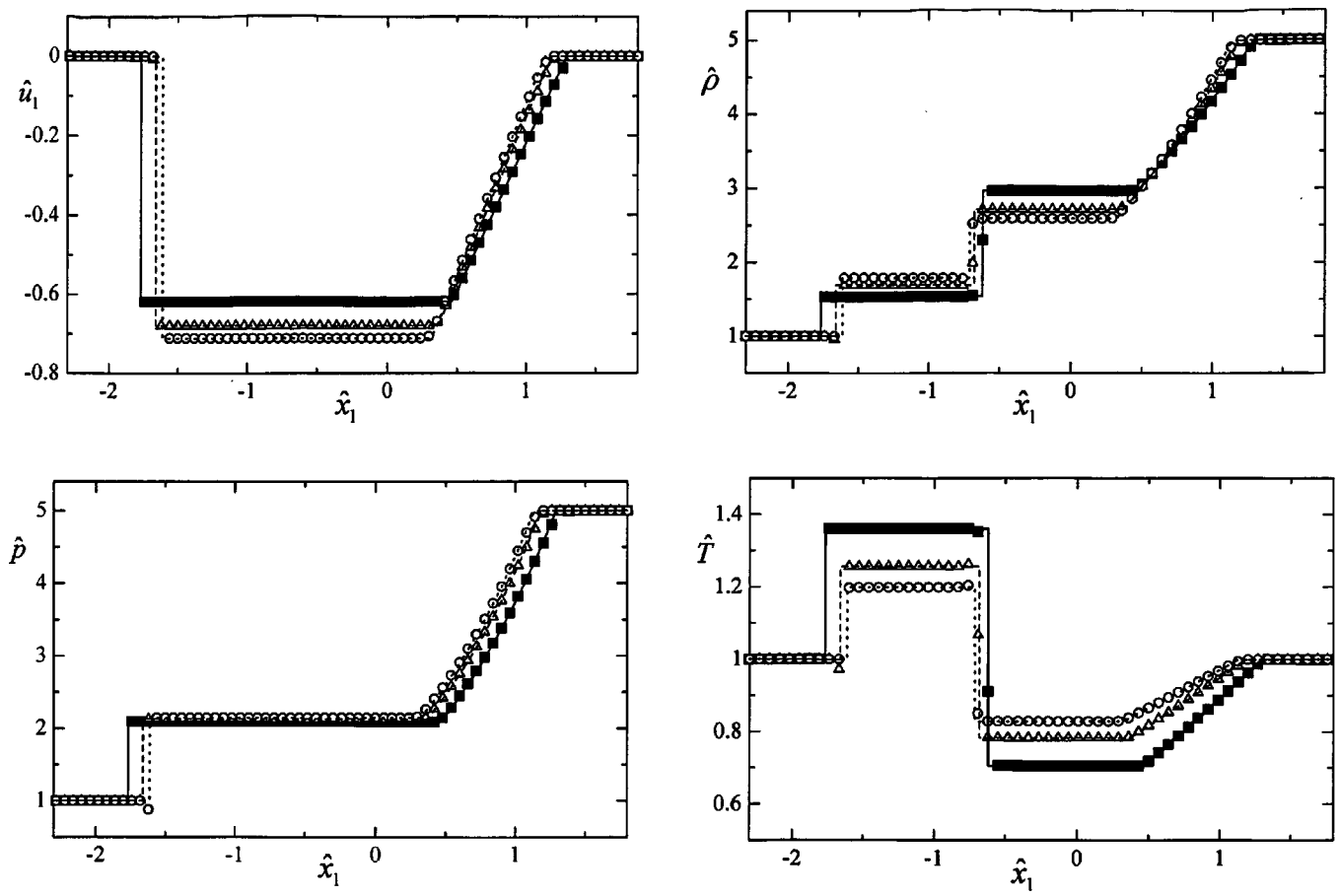

FIG. 6. The $\hat{x}_1$ dependence of $\hat{u}_1$, $\hat{p}$, $\hat{\rho}$, and $\hat{T}$ of the results by the LBM for the one-dimensional problem whose initial condition is Eq. (48) with $\varepsilon=10^{-4}$ and $P=5$. The plots are the results by the LBM with $\Delta\hat{x}=0.002$: ■, $\gamma=5/3$; △, $\gamma=7/5$; ◯, $\gamma=9/7$. The lines represent the corresponding theoretical solutions for $\gamma=5/3$ (solid lines), $7/5$ (dashed lines), and $9/7$ (dotted lines).

across which the entropy of fluid particles decreases (or waves across which the pressure of fluid particles decreases) in all the obtained numerical results including the two- and three-dimensional flows which are not shown here. Thus, we believe that the scheme used in the present study [the usual finite-difference scheme with the first-order forward in time and the second-order upwind in space of the kinetic equation (15)] can describe the shock wave propagation correctly with the entropy condition being satisfied. Third, the lattice Boltzmann models including our model can cause numerical instability if the local Mach number exceeds 1. The precise mechanism of this instability has not yet been clarified, and there are some opinions, e.g., the velocity distribution function being negative values. However, we found that stable calculation is possible even with the negative velocity distribution function if the local Mach number does not exceed 1. The reason for this numerical instability is, therefore, a pending problem of the lattice Boltzmann method that should be clarified.

V. CONCLUSION

The lattice Boltzmann model for the compressible Euler equations that can take the flexible specific-heat ratio with

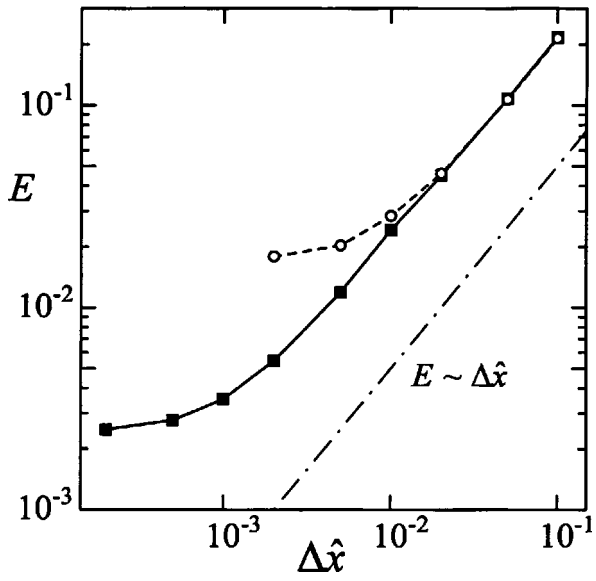

FIG. 7. The $\Delta\hat{x}$ dependence of E for the numerical results of the one-dimensional problem whose initial condition is given by Eq. (48) with $P=5$ and $\gamma=5/3$: ◯, $\varepsilon=10^{-3}$; ■, $\varepsilon=10^{-4}$. The dash-dot line in the figure represents $E\sim\Delta\hat{x}$.

small number of discrete velocities is presented together with its rigorous theoretical background. First, we treated the case where the solution makes an appreciable variation over the length or time scale of the system. Then the macroscopic variables obtained from the solution of the kinetic equation (15) and the initial condition (16) satisfy the compressible Euler equations and their initial condition. In contrast, when the scale of variation is steep due to shock waves and contact discontinuities at some local regions, the macroscopic variables obtained from the solution of the integral relation (40) satisfy the weak form of the compressible Euler equations. Numerical examples and the error estimates are also presented, and the results supported the above theoretical arguments.

APPENDIX: CONSISTENCY OF THE FINITE-DIFFERENCE SCHEME WITH THE INTEGRAL RELATION (40)

In this appendix, we will prove that the usual finite-difference scheme with $\Delta\hat{t}\sim\varepsilon$ and $\Delta\hat{x}\sim\varepsilon$ of the kinetic equation (15) ($D=1$) and the initial condition (16) is consistent with the integral relation (40) (see also Ref. [14]). For the sake of simplified discussion and notations, the first-order scheme is considered and the caret notation is omitted. The extensions to the multidimensions ($D=2,3$) and the higher-order schemes are straightforward. We start with the following finite-difference scheme of the kinetic equation (15) ($D=1$) and the initial condition (16):

$$\frac{f_i(t+\Delta t,x)-f_i(t,x)}{\Delta t}+c_i\frac{f_i(t,x)-f_i(t,x-\Delta x)}{\Delta x}=\frac{f_i^{\mathrm{eq}}(\rho,u,T)-f_i(t,x)}{\varepsilon}, \tag{A1}$$

$$f_i(0,x)=f_i^{\mathrm{eq}}(\rho^0,u^0,T^0). \tag{A2}$$

Multiplying Eq. (A1) by $\psi(t,x)$, or any smooth test function of t and x that vanishes for $t+|x|$ large enough, and integrating over the whole $t-x$ plane, we obtain

$$\int_{-\infty}^{\infty}dx\int_0^{\infty}\left[\left(\frac{f_i(t+\Delta t,x)-f_i(t,x)}{\Delta t}+c_i\frac{f_i(t,x)-f_i(t,x-\Delta x)}{\Delta x}-\frac{f_i^{\mathrm{eq}}(\rho,u,T)-f_i(t,x)}{\varepsilon}\right)\psi(t,x)\right]dt=0. \tag{A3}$$

Transforming the term involving $f(t+\Delta t,x)$ on the left-hand side by replacing the variable of integration $t+\Delta t$ by t, and the term involving $f(t,x-\Delta x)$ by replacing the variable $x-\Delta x$ by x, we get

$$\int_{-\infty}^{\infty}dx\int_0^{\infty}\left[\left(\frac{\psi(t-\Delta t,x)-\psi(t,x)}{\Delta t}+c_i\frac{\psi(t,x)-\psi(t,x+\Delta x)}{\Delta x}\right)f_i(t,x)-\frac{f_i^{\mathrm{eq}}(\rho,u,T)-f_i(t,x)}{\varepsilon}\psi(t,x)\right]dt-\int_{-\infty}^{\infty}dx\int_0^{\Delta t}\frac{\psi(t-\Delta t,x)f_i(t,x)}{\Delta t}dt=0. \tag{A4}$$

The difference of $\psi(t-\Delta t,x)f_i(t,x)(0<t<\Delta t)$ and $\psi(0,x)f_i(0,x)$ is of the order of unity only in the regions of $O(\varepsilon)+O(\Delta x)$ where the initial value of f_i makes a steep variation, and it is $O(\Delta t)$ in the other regions where the initial value of f_i makes a moderate variation. Thus, the last term on the left-hand side of Eq. (A4) becomes

$$\begin{aligned}-\int_{-\infty}^{\infty}dx\int_0^{\Delta t}\frac{\psi(t-\Delta t,x)f_i(t,x)}{\Delta t}dt&=-\int_{-\infty}^{\infty}\psi(0,x)f_i(0,x)dx+O(\varepsilon)+O(\Delta x)+O(\Delta t)\\&=-\int_{-\infty}^{\infty}\psi(0,x)f_i^{\mathrm{eq}}(\rho^0,u_\alpha^0,T^0)dx+O(\varepsilon)+O(\Delta x)+O(\Delta t),\end{aligned} \tag{A5}$$

where the initial condition (A2) is used to derive the far right side. Then, from Eq. (A4),

$$\int_{-\infty}^{\infty}dx\int_0^{\infty}\left[\left(\frac{\psi(t,x)-\psi(t-\Delta t,x)}{\Delta t}+c_i\frac{\psi(t,x+\Delta x)-\psi(t,x)}{\Delta x}\right)f_i(t,x)+\frac{f_i^{\mathrm{eq}}(\rho,u,T)-f_i(t,x)}{\varepsilon}\psi(t,x)\right]dt+\int_{-\infty}^{\infty}\psi(0,x)f_i^{\mathrm{eq}}(\rho^0,u_\alpha^0,T^0)dx=O(\varepsilon)+O(\Delta x)+O(\Delta t). \tag{A6}$$

As $\Delta t\sim\varepsilon$ and $\Delta x\sim\varepsilon$ tend to zero, then, Eq. (A6) converges to the integral relation (40). Thus, the consistency of the finite-difference scheme ($\Delta t\sim\varepsilon$ and $\Delta x\sim\varepsilon$) with the integral relation (40) has been proved.

We can easily extend the above discussion to the scheme (8) often used in the LBM, and also to the higher-order finite-difference schemes.

[1] G. Yan, Y. Chen, and S. Hu, Phys. Rev. E **59**, 454 (1999).
[2] Y. H. Qian, J. Sci. Comput. **8**, 231 (1993).
[3] Y. Chen, H. Ohashi, and M. Akiyama, Phys. Rev. E **50**, 2776 (1994).
[4] F. J. Alexander, S. Chen, and J. D. Sterling, Phys. Rev. E **47**, 2249 (1993).
[5] Y. H. Qian and S. A. Orszag, Europhys. Lett. **21**, 255 (1993).
[6] M. B. Reider and J. D. Sterling, Comput. Fluids **24**, 459 (1995).
[7] Y. H. Qian, D. d'Humiēres, and P. Lallemand, Europhys. Lett. **17**, 479 (1992).
[8] S. Chen and G. D. Doolen, Annu. Rev. Fluid Mech. **30**, 329 (1998).
[9] T. Inamuro, M. Yoshino, and F. Ogino, Phys. Fluids **9**, 3535 (1997).
[10] L. D. Landau and E. M. Lifshitz, *Fluid Mechanics*, 2nd ed. (Pergamon, Oxford, 1987).
[11] T. Ohwada, Phys. Fluids A **5**, 217 (1993).
[12] P. D. Lax, Commun. Pure Appl. Math. **7**, 159 (1954).
[13] P. D. Lax, Commun. Pure Appl. Math. **10**, 537 (1957).
[14] P. D. Lax and B. Wendroff, Commun. Pure Appl. Math. **13**, 217 (1960).
[15] Y. Sone, J. Jpn. Soc. Fluid Mech. **6**, 182 (1987) (in Japanese).
[16] Y. Sone and K. Aoki, *Molecular Gas Dynamics* (Asakura, Tokyo, 1994) (in Japanese).
[17] Y. Sone, *Kinetic Theory and Fluid Dynamics* (Birkhäuser, Boston, 2002).
[18] T. Kataoka and M. Tsutahara, Phys. Rev. E **69**, 035701(R) (2004).
[19] P. L. Bhatnagar, E. P. Gross, and M. Krook, Phys. Rev. **94**, 511 (1954).
[20] R. McNamara, A. L. Garcia, and B. J. Alder, J. Stat. Phys. **81**, 395 (1995).
[21] N. Cao, S. Chen, S. Jin, and D. Martinez, Phys. Rev. E **55**, 21 (1997).
[22] D. Hilbert, *Grundzüge einer Allgemeinen Theorie der Linearen Integralgleichungen* (Teubner, Leipzig, 1912).
[23] H. W. Liepmann and A. Roshko, *Elements of Gasdynamics* (Wiley, New York, 1957).
[24] R. W. MacCormack, AIAA Pap. **69**, 354 (1969).
[25] J. J. Gottlieb and C. P. T. Groth, J. Comput. Phys. **78**, 437 (1988).